Electromagnetically induced transparency and dark fluorescence in a cascade three-level diatomic lithium system

Jianbing Qi[1] and A. Marjatta Lyyra[2]
[1]*Department of Physics and Astronomy, Penn State Berks, Tulpehocken Road, P.O. Box 7009, Reading, Pennsylvania 19610, USA*
[2]*Physics Department, Temple University, Philadelphia, Pennsylvania 19112, USA*
(Received 20 September 2005; published 19 April 2006)

Following our previous brief report [Phys. Rev. Lett. **88**, 173003 (2002)], we report here a detailed study of electromagnetically induced transparency (EIT) and dark fluorescence in a cascade three-level diatomic lithium system using optical-optical double resonance (OODR) spectroscopy for both resonance and off resonance coupling. When a strong coupling laser couples the intermediate state $A\ ^1\Sigma_u^+(v=13,J=14)$ to the upper state $G\ ^1\Pi_g(v=11,J=14)$ of $^7Li_2$, the fluorescence from both $A\ ^1\Sigma_u^+$ and $G\ ^1\Pi_g$ states was drastically reduced as the weak probe laser was tuned through the resonance transition between the ground state $X\ ^1\Sigma_g^+(v=4,J=15)$ and the excited state $A\ ^1\Sigma_u^+(v=13,J=14)$. The strong coupling laser makes an optically thick medium transparent for the probe transition. In addition, the fact that fluorescence from the upper state $G\ ^1\Pi_g(v=11,J=14)$ was also dark when both lasers were tuned at resonance implies that the molecules were trapped in the ground state. We used density matrix methods to simulate the response of an open molecular three-level system to the action of a strong coupling field and a weak probe field. The analytical solutions were obtained under the steady-state condition. We have incorporated the magnetic sublevel (M) degeneracy of the rotational levels in the line shape analysis and report $|M|$ dependent line shape splitting. Our theoretical calculations are in excellent agreement with the observed fluorescence spectra. We show that the coherence is remarkably preserved even when the coupling field was detuned far from the resonance.

DOI: 10.1103/PhysRevA.73.043810 PACS number(s): 42.50.Gy, 42.50.Hz, 33.40.+f

I. INTRODUCTION

Multilevel atomic and molecular systems offer many possibilities for the investigation of coherence effects and quantum control of the interactions among the quantum participants. In recent years, substantial attention has been paid to the study of coherence effects in atomic and molecular systems [1–4], such as coherent population trapping (CPT) [5–7], electromagnetically induced transparency (EIT) [8–11], ultraslow propagation of light [12,13], and Autler-Townes splitting [14–17]. More and more experiments are shifted from atomic systems to molecular systems for more practical applications [18,19]. The multitude of quantum levels of molecular systems provides rich coupling schemes and thus a test ground for the study of coherence effects in molecular systems. However, compared to atomic systems, molecules have small transition dipole moments. A general characteristic of molecular systems is that they have many relaxation pathways. This in turn makes these systems much more open compared to closed atomic systems where excited states decay channels are limited. The degeneracy of ground state and the role of the different hyperfine transitions in an atomic sodium CPT experiments were discussed by Renzoni *et al.* [20]. They demonstrated that CPT can be realized on the open transitions but with less efficiency when the optical pumping into hyperfine levels external to those of the excited transition is increased. Furthermore, the degeneracy of the energy levels and other complications make the observation of coherence effects considerably more challenging from an experimental point of view. The Rabi frequency, the key parameter, is proportional to the transition dipole moment matrix element and the coupling field amplitude. Thus cw laser experiments that involve small transition dipole moment matrix elements are therefore quite difficult. However, a judicious choice of laser wavelengths and beam propagation geometry can help overcome the Doppler broadening [21]. The Autler-Townes splitting was demonstrated in pulsed laser experiments on the H_2 molecule [22], and was observed in a high-temperature diatomic lithium gas using multiple resonance excitation to overcome the Doppler effect [16,23]. Our cw experiments show that we can investigate coherence effects by using laser sources with moderate output power and avoid the complications that arise with high power laser sources such as multiphoton ionization leading to a loss of the neutral molecules being studied. In addition, the accuracy and the resolution achieved in cw experiments are much higher than in pulsed laser experiments. Recently, EIT in ultracold atomic gases, and Autler-Townes splitting effect in ultracold molecule formation and detection have been reported [24–26]. The study of coherence effects in molecular systems is timely and important not only for fundamental understanding of these effects, but also for the practical applications. In this paper, we present a detailed experimental investigation and the corresponding theoretical analysis of electromagnetically induced transparency and dark fluorescence in a cascade three-level diatomic lithium in an inhomogeneously broadened sample. We have incorporated the effect of the magnetic sublevel (M) degeneracy of the rotational levels in the line shape analysis and report $|M|$-dependent line shape splitting. We included the transverse motion of the molecule in our new theoretical calculations. This is important for cases when the laser beams are tightly focused and the transient rate cannot be neglected whenever it is comparable with the radiative decay rate of

the excited states. In our case, the radiative decay rate of the excited states (~9.85 MHz for the intermediate level and ~15.9 MHz for the upper level) is about five to eight times the transient rate (~2 MHz), but the inclusion of the transient rate in our new calculations improves the fitting of the experimental spectra in an obvious manner. We show that the coherence is remarkably preserved even when the coupling field was detuned far from the resonance. However, a closed three-level model such as in Ref. [22] is not capable to explain the experimental results for our system. An open three-level model is introduced in our theory, which can simulate the experimental spectra very well. The open property of molecular systems will be discussed in our theoretical calculations. We also demonstrated that the coupling laser field dependent splitting of the upper level can be used as a new method for measuring the molecular transition dipole moment matrix element [23].

The paper is organized as follows. In Sec. II, we present the theoretical model and the derivation of the analytical expressions to account for the experiments. We describe the experimental observations in Sec. III. The discussion of the theoretical calculations using the experimental parameters is given in Sec. IV. Finally, a summary is presented.

II. THEORETICAL FRAMEWORK

A. Density matrix equation of motion

The excitation scheme for a three-level molecular system interacting with two laser fields is indicated in Fig. 1(a). We consider a moving molecule situated in a traveling wave $\vec{E}_i(z,t)=\vec{e}_i E_i \cos(k_i z-\omega_i t)$. The Hamiltonian H is given by

$$H = H_0 + H_{\text{int}}, \tag{1}$$

where

$$H_0 = \sum_{i=1}^{3} \varepsilon_i |i\rangle\langle i| \tag{2}$$

is the molecular Hamiltonian, and ε_i is the energy eigenvalue of the isolated molecule in state $|i\rangle$. We assume $\varepsilon_1=0$ for simplicity and all other states are measured relative to state $|1\rangle$. The

$$H_{\text{int}} = \sum_{i\neq j} \langle i|-\vec{\mu}\cdot\vec{E}|j\rangle = -\sum_{i\neq j} \mu_{ij} E_i \tag{3}$$

is the dipole interaction Hamiltonian, and μ_{ij} is the transition dipole moment for a molecule undergoing $|i,v',J'\rangle \leftrightarrow |j,v,J\rangle$ transition. The evolution of the molecular density matrix for a molecule moving with velocity v is governed by the master equation [27]

$$\frac{\partial \varrho}{\partial t} + \vec{v}\cdot\vec{\nabla}\varrho = -\frac{i}{\hbar}[H,\varrho] + \left(\frac{\partial \varrho}{\partial t}\right)_{\text{inc}}, \tag{4}$$

where the second term on the left hand-side represents the damping due to spontaneous emission and other irreversible processes.

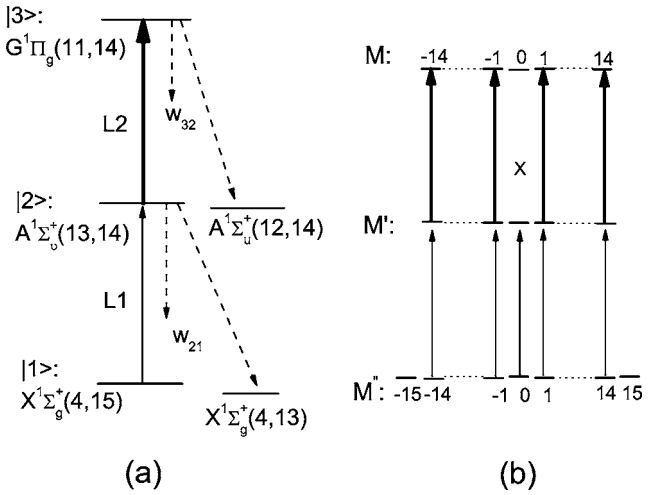

FIG. 1. $^7Li_2$ three-level cascade scheme. (a) The weak probe laser $L1$ (15642.636 cm^{-1}) was used to excite molecules from the ground state level $X\,^1\Sigma_g^+(v=4,J=15)$ to an excited intermediate level $A\,^1\Sigma_u^+(v=13,J=14)$. The laser, $L2$ (17053.954 cm^{-1}), coupled the intermediate level to a higher electronic state level $G\,^1\Pi_g(v=11,J=14)$. The fluorescence from $A\,^1\Sigma_u^+(v=13,J=14)$ to $X\,^1\Sigma_g^+(v=4,J=13)$ and $G\,^1\Pi_g$ to $A\,^1\Sigma_u^+(v=12,J=14)$ were monitored. (b) The coupling details of the magnetic sublevels ($M=-J, -J-1,\ldots,J-1,J$) of (a): For linearly polarized light, the selection rules require $\Delta M=0$, thus The $M''=\pm 15$ of the ground state levels are decoupled from the first transition (P transition: $\Delta J=-1$), while there is no $M=0\rightarrow M'=0$ coupling for the upper transition (Q transition: $\Delta J=0$).

Before we apply the density matrix formalism to interpret the experimental results, we have to consider the relaxation details of the level system in Fig. 1(a). The first laser $L1$ excites the $^7Li_2$ molecules from the ground state level $X\,^1\Sigma_g^+(v=4,J=15)$ (level $|1\rangle$) to the intermediate level $A\,^1\Sigma_u^+(v=13,J=14)$ (level $|2\rangle$), and the second laser $L2$ couples the $A\,^1\Sigma_u^+(v=13,J=14)$ to the upper excited state $G\,^1\Pi_g(v=11,J=14)$ (level $|3\rangle$). Molecules in any specific rovibrational level of an excited electronic state can decay to many other rovibrational levels of lower electronic states, and only part of them decay back to their initial state. The upper excited electronic state $G\,^1\Pi_g$ can decay to two lower electronic states of $B\,^1\Pi_u$ and $A\,^1\Sigma_u^+$. The $A\,^1\Sigma_u^+$ state is the first singlet excited electronic state of the lithium dimer molecule. Molecules in a rovibrational level of the $A\,^1\Sigma_u^+$ state can decay to vibrational levels of the ground electronic state $X\,^1\Sigma_g^+$. In the sense of the description of the total decay rate of level $|3\rangle$ to other energy levels, there is no difference between $B\,^1\Pi_u$ and $A\,^1\Sigma_u^+$ state.

We assume that the total radiative decay rate of the excited states $|2\rangle$ and $|3\rangle$ are γ_2 and γ_3, respectively. The branching ratios b_2 and b_3 stand for the percentage of molecules in the level $|2\rangle$ and the level $|3\rangle$ that decay back to the ground state $|1\rangle$ and level $|2\rangle$, respectively. When the branching ratios are equal to unity the three-level system is closed. The laser frequency detunings for a stationary molecule are defined as

$$\delta_1 = \omega_1 - \omega_{21} \tag{5}$$

and

$$\delta_2 = \omega_2 - \omega_{32}, \tag{6}$$

where $\omega_{ij}=(\varepsilon_i-\varepsilon_j)/\hbar$ is the resonance transition frequency between $|i\rangle$ and $|j\rangle$. The Rabi frequency of the corresponding laser field is defined as

$$g_i = \mu_{ij}E_i/\hbar. \tag{7}$$

We assume that the population of the ground state $|1\rangle$ has been replenished at the rate Λ, and only the ground state is replenished. The laser beam has a finite beam size and therefore the transverse motion of molecules can remove molecules from the interaction region before decay. This will introduce an effective additional relaxation of the excited states and the ground state. In order to account for this transit time, we simulate it with an effective decay rate $w(w \ll \gamma_i)$ for all populations and polarizations. Then, the explicit form of Eq. (4) is

$$\left(\frac{\partial}{\partial t} + v_z\frac{\partial}{\partial z}\right)\varrho_{33} = ig_2\cos(k_2z-\omega_2t)(\varrho_{32}-\varrho_{23}) - (\gamma_3+w)\varrho_{33}, \tag{8}$$

$$\left(\frac{\partial}{\partial t} + v_z\frac{\partial}{\partial z}\right)\varrho_{22} = -ig_2\cos(k_2z-\omega_2t)(\varrho_{32}-\varrho_{23}) - ig_1\cos(k_1z-\omega_1t)(\varrho_{12}-\varrho_{21}) + W_{32}\varrho_{33} - (\gamma_2+w)\varrho_{22}, \tag{9}$$

$$\left(\frac{\partial}{\partial t} + v_z\frac{\partial}{\partial z}\right)\varrho_{11} = ig_1\cos(k_1z-\omega_1t)(\varrho_{12}-\varrho_{21})$$

$$\Lambda + W_{21}\varrho_{22} - w\varrho_{11}, \tag{10}$$

$$\left(\frac{\partial}{\partial t} + v_z\frac{\partial}{\partial z}\right)\varrho_{32} = ig_2\cos(k_2z-\omega_2t)(\varrho_{33}-\varrho_{22}) + (-i\omega_{32}-\gamma_{32}-w)\varrho_{32} + ig_1\cos(k_1z-\omega_1t)\varrho_{31}, \tag{11}$$

$$\left(\frac{\partial}{\partial t} + v_z\frac{\partial}{\partial z}\right)\varrho_{31} = [-i\omega_{31}-(\gamma_{31}+w)]\varrho_{31} - ig_2\cos(k_2z-\omega_2t)\varrho_{21} + ig_1\cos(k_1z-\omega_1t)\varrho_{32}, \tag{12}$$

$$\left(\frac{\partial}{\partial t} + v_z\frac{\partial}{\partial z}\right)\varrho_{21} = [-i\omega_{21}-(\gamma_{21}+w)]\varrho_{21} + ig_1\cos(k_1z-\omega_1t)(\varrho_{22}-\varrho_{11}) - ig_2\cos(k_2z-\omega_2t)\varrho_{31}, \tag{13}$$

where the W_{ij} is the population decay rate from level $|i\rangle$ to $|j\rangle$, $W_{32}=b_3\gamma_3$, and $W_{21}=b_2\gamma_2$, and γ_{ij}^c represents the collisional dephasing rate. The polarization decay rate γ_{ij} is given by

$$\gamma_{ij} = \gamma_{ji} = \frac{1}{2}(\gamma_i+\gamma_j) + \gamma_{ij}^c.$$

Let

$$\Delta_1 = \omega_1 - \omega_{12} - k_1v_z = \delta_1 - k_1v_z \tag{14}$$

and

$$\Delta_2 = \omega_2 - \omega_{23} - k_2v_z = \delta_2 - k_2v_z, \tag{15}$$

where v_z is the velocity component of the molecule in the laser propagation direction. Equations (8)–(13) can be changed into ones for the density-matrix elements of the slowly varying function of time and space by setting

$$\varrho_{21} = \rho_{21}e^{i(k_1z-\omega_1t)}, \tag{16}$$

$$\varrho_{32} = \rho_{32}e^{i(k_2z-\omega_2t)}, \tag{17}$$

$$\varrho_{31} = \rho_{31}e^{i[(k_1+k_2)z-(\omega_1+\omega_2)t]}. \tag{18}$$

After applying the rotating wave approximation, the above equations (8)–(13) can be written as

$$\frac{d\rho_{33}}{dt} = i\frac{g_2}{2}(\rho_{32}-\rho_{23}) - (\gamma_3+w)\rho_{33}, \tag{19}$$

$$\frac{d\rho_{22}}{dt} = i\frac{g_1}{2}(\rho_{21}-\rho_{12}) - i\frac{g_2}{2}(\rho_{32}-\rho_{23}) - (\gamma_2+w)\rho_{22} + W_{32}\rho_{33}, \tag{20}$$

$$\frac{d\rho_{11}}{dt} = i\frac{g_1}{2}(\rho_{12}-\rho_{21}) + W_{21}\rho_{22} - w\rho_{11} + \Lambda, \tag{21}$$

$$\frac{d\rho_{32}}{dt} = i\frac{g_2}{2}(\rho_{33} - \rho_{22}) + i\frac{g_1}{2}\rho_{31} + i\Delta_2\rho_{32} - (\gamma_{23} + w)\rho_{32}, \tag{22}$$

$$\frac{d\rho_{31}}{dt} = i\frac{g_1}{2}\rho_{32} - i\frac{g_2}{2}\rho_{21} - (\gamma_{13} + w)\rho_{31} + i(\Delta_1 + \Delta_2)\rho_{31}, \tag{23}$$

$$\frac{d\rho_{21}}{dt} = i\frac{g_1}{2}(\rho_{22} - \rho_{11}) - i\frac{g_2}{2}\rho_{31} + i\Delta_1\rho_{21} - (\gamma_{12} + w)\rho_{21}, \tag{24}$$

In the steady-state limit, we can solve the above equations iteratively for the population (ρ_{ii}) of each level to the lowest order of the weak probe laser Rabi frequency g_1, but to all orders in g_2. After some lengthy algebra, we obtain the non-normalized analytical solutions for the populations of the two excited states:

$$\rho_{22} = -\frac{g_1^2\rho_{11}^{(0)}}{2D(\Delta_2)}\,\mathrm{Im}\left\{\frac{\frac{g_2^2}{4}\left(1 - \frac{W_{32}}{\gamma_3 + w}\right)[\Delta_2 - i(\gamma_{32} + w)] + A[\Delta_1 + \Delta_2 + i(\gamma_{31} + w)]}{[\Delta_1 + i(\gamma_{21} + w)][\Delta_1 + \Delta_2 + i(\gamma_{31} + w)] - \frac{g_2^2}{4}}\right\} \tag{25}$$

and

$$\rho_{33} = \frac{g_1^2 g_2^2 \rho_{11}^{(0)}}{8D(\Delta_2)(\gamma_3 + w)}\,\mathrm{Im}\left\{\frac{-2(\gamma_{32} + w)[\Delta_1 + \Delta_2 + i(\gamma_{31} + w)] + (\gamma_2 + w)[\Delta_2 - i(\gamma_{32} + w)]}{[\Delta_1 + i(\gamma_{21} + w)][\Delta_1 + \Delta_2 + i(\gamma_{31} + w)] - \frac{g_2^2}{4}}\right\}, \tag{26}$$

where

$$A = \Delta_2^2 + (\gamma_{32} + w)^2 + \frac{g_2^2(\gamma_{32} + w)}{2(\gamma_3 + w)},$$

$$D(\Delta_2) = A(\gamma_2 + w) + \frac{g_2^2(\gamma_{23} + w)}{2}\left(1 - \frac{W_{32}}{\gamma_3 + w}\right),$$

and $\rho_{11}^{(0)} = \frac{\Lambda}{w}$ is the initial population without the probe laser field. We can see that the system will be ideally closed if $W_{32} = \gamma_3 + w$, and the expressions will be greatly simplified.

B. Doppler effect

Let us assume that two laser beams counter propagate along the z axis, the probe laser travels to the right (positive), and the coupling laser to the left (negative). Due to the Doppler effect, a molecule moving with a positive velocity v_z with respect to the rest frame will *see* the probe laser and coupling laser frequencies ω_1 and ω_2, respectively, as

$$\omega_1(v_z) = \omega_1 - \frac{v_z}{c}\omega_1 \tag{27}$$

and

$$\omega_2(v_z) = \omega_2 + \frac{v_z}{c}\omega_2. \tag{28}$$

We define the velocity dependent detunings as

$$\Delta_1(v_z) = \delta_1 - \frac{v_z}{c}\omega_1 \tag{29}$$

and

$$\Delta_2(v_z) = \delta_2 + \frac{v_z}{c}\omega_2. \tag{30}$$

The velocity dependent laser detunings can be expressed in laser frequency detuning and the transition frequency as follows:

$$\Delta_1(v_z) = \left(1 - \frac{v_z}{c}\right)\delta_1 - \frac{v_z}{c}\omega_{12} \tag{31}$$

and

$$\Delta_2(v_z) = \left(1 + \frac{v_z}{c}\right)\delta_2 + \frac{v_z}{c}\omega_{23}. \tag{32}$$

At thermal equilibrium, the molecules in gas phase follow the Maxwellian velocity distribution, in one dimension, which is given as [28]

$$N(v_z) = \frac{1}{\sqrt{\pi}u_p}\exp\left(-\frac{v_z^2}{u_p^2}\right), \tag{33}$$

where $u_p = (2kT/m)^{1/2}$ is the most probable velocity of the molecules, k is the Boltzmann's constant, m is the mass of a molecule, and T is the temperature. The experimental observations should be the sum ρ_{ii} for all velocity groups:

$$\langle \rho_{ii} \rangle_{\text{Doppler}} = \int_{-\infty}^{+\infty} \rho_{ii} N(v_z) dv_z. \tag{34}$$

C. $|M|$-dependent Rabi frequency

For each rotational angular momentum J, there are $2J+1$ magnetic sublevels, $M=-J,-(J-1),\ldots,J-1,J$, which specify the projection of the total angular momentum J along a laboratory fixed Y axis. The interaction of each magnetic sublevel with the laser field depends not only on the transition (P, Q, or R) but also on the polarization of the laser field [29,30]. The Rabi frequency g_i for each laser field and for a given molecular transition of $(v',J') \leftarrow (v,J)$ can be written in the form

$$g_i = \mu_{ij} E_i/\hbar = \langle v'|\mu_e|v\rangle f(J'JM'M;\Lambda'\Lambda) E_i/\hbar, \tag{35}$$

where μ_e is the electronic transition dipole moment, $\mu_e = \langle \Lambda'|\mu|\Lambda\rangle$, $f(J'JM'M;\Lambda'\Lambda)$ is the rotational line strength factor for transition $|J'M'\Lambda'\rangle \leftrightarrow |JM\Lambda\rangle$, and E_i is the laser field strength. For a linearly polarized laser field, the rotational line strength factor for the $Q(\Delta J = J - J' = 0)$ transition is

$$f_Q = \frac{|M|}{\sqrt{J(J+1)}} \tag{36}$$

and for the $P(\Delta J = J - J' = -1)$ transition

$$f_P = \sqrt{\frac{(J^2 - M^2)}{(2J+1)(2J-1)}}. \tag{37}$$

For linearly polarized light, the transition selection rules require $\Delta M = M' - M = 0$, thus there is no $M=0 \rightarrow M'=0$ coupling for upper transition. The $M''=\pm 15$ of the ground state are decoupled from the first transition also. The coupling of the three-level configuration of the Fig. 1(a) can be viewed as 28 M-dependent couplings for $L2$ and 29 couplings for $L1$, as shown in Fig. 1(b). The Rabi frequency depends on the absolute value of the magnetic sublevel $|M|$. This results in $|M|$-dependent population expressions of Eqs. (25) and (26) also. The observed fluorescence signal, apart from a proportionality factor, can be calculated by integrating the ρ_{ii} over the velocity distribution and summing over all $|M|$, i.e.,

$$\rho_{ii}(\delta_1, \delta_2) \propto \sum_{|M|} \int_{-\infty}^{+\infty} \rho_{ii} N(v_z) dv_z. \tag{38}$$

III. EXPERIMENTAL RESULTS

The experimental setup is shown in Fig. 2. This is a typical optical-optical double resonance (OODR) scheme. Lithium dimer molecules are generated in a five-arm stainless steel oven with the temperature around 1000 K, and with argon buffer gas pressure around 100–300 mTorr. Two Coherent 699-29 Autoscan dye lasers were used to produce the required laser wavelengths. Two linearly polarized laser beams were arranged in counterpropagating configuration and aligned coaxially.

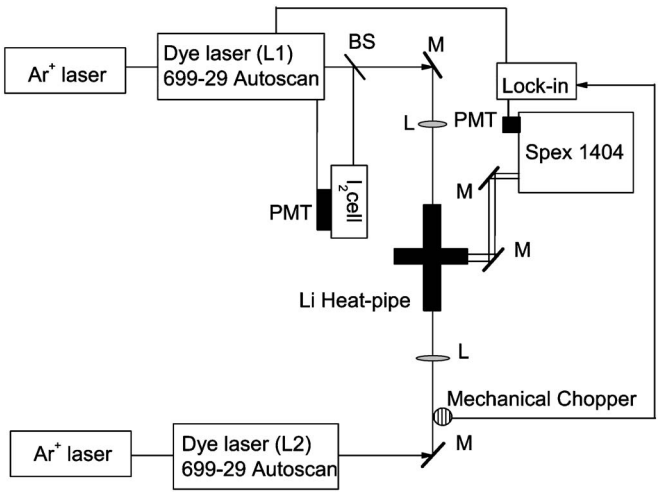

FIG. 2. Experimental setup: Two linearly polarized counterpropagating laser beams were aligned coaxially, and were focused at the center of the lithium heat pipe. The fluorescence was collected and focused to the monochromator (SPEX 1404) from the side window. The signal was amplified by the lock-in amplifier and the output was recorded on the Coherent 699-29 Autoscan computer. (M: Mirror, BS: Beam splitter, L: Lens, PMT: Photomultiplier.)

We monitored the population of the intermediate state $A\,^1\Sigma_u^+(v=13,J=14)$ (level $|2\rangle$) by detecting its fluorescence to the ground-state rovibrational level $X\,^1\Sigma_g^+(v=4,J=13)$. The corresponding wavelength is 6377.83 Å in air. The population of the upper state $G\,^1\Pi_g(v=11,J=14)$ (level $|3\rangle$) was monitored by detecting its fluorescence to the $A\,^1\Sigma_u^+(v=12,J=14)$ state with the wavelength of 5791.30 Å in air. The fluorescence was collected and focused to the monochromator (SPEX 1404) through a set of mirrors from the side window of the heat-pipe oven. The selected fluorescence was detected by a cooled photomultiplier (PMT) at the exit slit of the SPEX when the monochromator was set to the corresponding spontaneous emission wavelength. The PMT signal was amplified by a lock-in amplifier (SR 850), and the output was recorded on the 699-29 Autoscan computer while the probe laser ($L1$) frequency was scanned. All laser frequencies were calibrated to $\pm 0.002\ \text{cm}^{-1}$ with the standard iodine spectra [31]. The first transition from the ground state level of $^7\text{Li}_2$ $X\,^1\Sigma_g^+(v=4,J=15)$ to the excited state $A\,^1\Sigma_u^+(v=13,J=14)$ is driven by the probe laser $L1$, while the transition from $A\,^1\Sigma_u^+(v=13,J=14)$ to the upper state level $G\,^1\Pi_g(v=11,J=14)$ is driven by laser $L2$. In the absence of laser $L2$, a frequency scan of the probe laser $L1$ yields the usual Doppler broadened fluorescence spectrum of the $A\,^1\Sigma_u^+(v=13,J=14)$ as shown in the Fig. 3(a). If the coupling laser $L2$ is weak and set at the resonance transition of the $A\,^1\Sigma_u^+(v=13,J=14)$ to $G\,^1\Pi_g(v=11,J=14)$, by monitoring the fluorescence of $G\,^1\Pi_g(v=11,J=14)$ to $A\,^1\Sigma_u^+(v=12,J=14)$, a scan of the probe laser from $X\,^1\Sigma_g^+(v=4,J=15)$ to $A\,^1\Sigma_u^+(v=13,J=14)$ leads to the usual OODR spectrum for the upper state, $G\,^1\Pi_g(v=11,J=14)$, as shown in Fig. 3(b). Upon increasing the coupling laser power, a sharp dip emerges at the center of the Doppler broadened fluores-

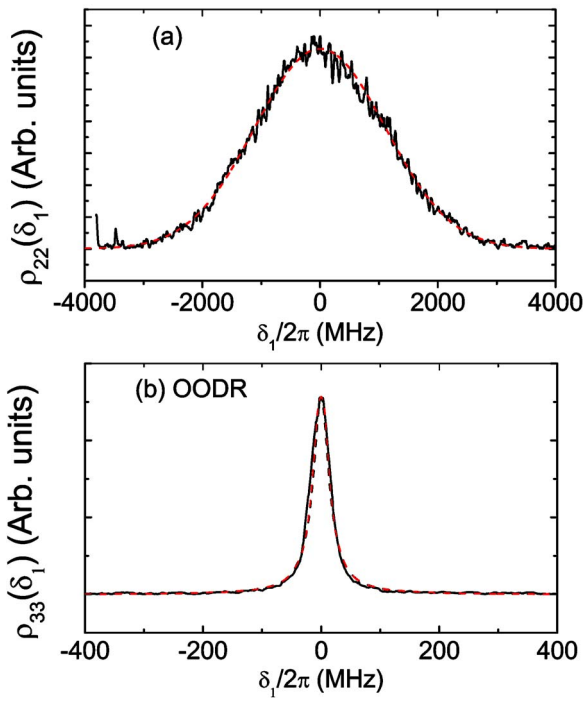

FIG. 3. (Color online) (a) The Doppler broadened fluorescence spectrum of $A\ ^1\Sigma_u^+(13,14)$ to $X\ ^1\Sigma_g^+(4,13)$ is plotted as a function of the detuning of the probe laser without the coupling laser. (b) Measured OODR signal of $G\ ^1\Pi_g(11,14)$ along with the calculation with 1 mW coupling laser power. (Solid lines: experiment, dashed lines: calculation.)

cence spectrum of the $A\ ^1\Sigma_u^+(v=13,J=14)$, as shown in Fig. 4(a). One may naively interpret the emergence of that dip as the consequence of the additional transfer of population to the upper level $G\ ^1\Pi_g(v=11,J=14)$ by the strong coupling laser. However, a sharp dip also appears in the middle of the OODR fluorescence signal of the upper $G\ ^1\Pi_g(v=11,J=14)$ level. The OODR fluorescence peak, splits into two components as shown in Fig. 4(b). The fluorescence of both excited states is drastically reduced under the action of the strong coupling laser ($L2$). Because the intensity of the fluorescence is proportional to the population of the corresponding excited state, the origin of the fluorescence dips is based on the fact that the molecules can not be excited by the probe laser and the coupling laser to either the intermediate level $A\ ^1\Sigma_u^+(v=13,J=14)$ or the upper level $G\ ^1\Pi_g(v=11,J=14)$ from the ground state under a strong coupling laser. Since the strong coupling laser $L2$ modified the transition from $X\ ^1\Sigma_g^+(v=4,J=15)$ to $A\ ^1\Sigma_u^+(v=13,J=14)$, the ground state molecules can not absorb the probe laser photons and be excited to the excited state $A\ ^1\Sigma_u^+(v=13,J=14)$ at the resonance frequency. The remarkable result is that the second transition does not transfer the molecules to the higher excited $G\ ^1\Pi_g$ state either. The experimental results also show that the stronger the coupling laser is, the deeper and wider are the dips as shown in Fig. 5. In a sense of the first transition, the molecule becomes transparent under the action of the strong coupling laser (electromagnetically induced transparency) and thus the molecules must stay in the ground state.

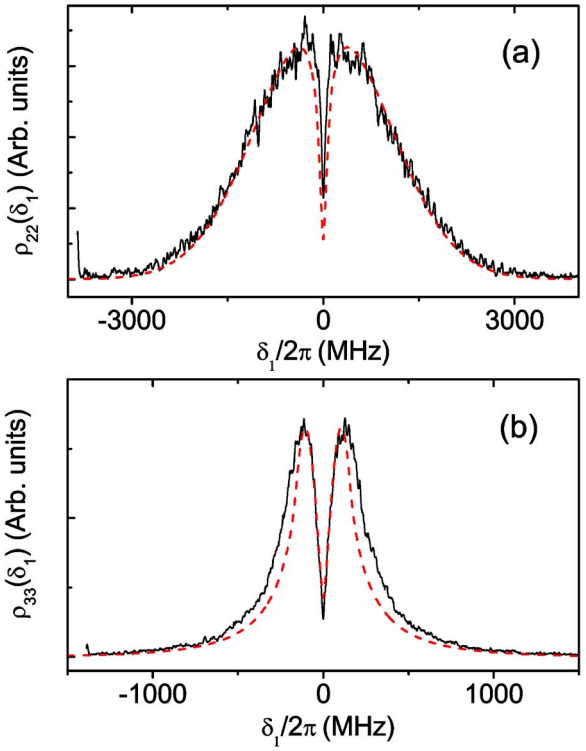

FIG. 4. (Color online) Measured experimental spectra along with the calculations. (a) Fluorescence from level $|2\rangle$. (b) Fluorescence from level $|3\rangle$. The fitting parameters are $\langle v'|\mu_e|v\rangle = 1.25(\pm 0.2)$ a.u., $\gamma_{13}^c/2\pi = \gamma_{23}^c/2\pi = 1$ MHz, $\gamma_{12}^c/2\pi = 5$ MHz. The coupling laser power is 480 mW. (Solid lines: experimental, dashed lines: calculation.)

IV. DISCUSSION

In order to carry out a comparison between the experimental spectra and the theory, we calculate Eq. (38) based on Eqs. (25) and (26) using the experimental data for the transition frequencies ω_{21} and ω_{32}. The lifetimes of level $|2\rangle$ ($\tau_2 = 1/\gamma_2$) and $|3\rangle$ ($\tau_3 = 1/\gamma_3$) were based on Refs. [32,33]. These values are 18 and 16.15 ns, respectively. From Fig. 3(a) (the probe laser scan) we obtained the most probable molecular velocity by measuring the Doppler linewidth, which is 2.6 GHz. The coupling beam waist ($1/e^2$) is 360 μm. The week probe laser beam is 222 μm (~1 mW). The transit rate (w) of the molecules entering and leaving the interaction region can be estimated according to Ref. [34] and is ~2 MHz. The branching ratios b_2 and b_3 can be estimated from the Franck Condon factor calculation to be 0.1 and 0.2, respectively. We perform the calculations based on the analytical solution of Eq. (26) by searching the value of the transition dipole moment matrix element and the γ_{ij}^c to best match the experimental spectrum of ρ_{33} in Fig. 4(b). The resulting value of the transition dipole moment matrix element $\langle v'|\mu_e|v\rangle$ for $G\ ^1\Pi_g - A\ ^1\Sigma_u^+$ is 1.25(±0.2) a.u. If the electronic transition dipole moment does not change violently in the region of the R centroid, we can write $\langle v'|\mu_e|v\rangle = \mu_e(R_c)\langle v'|v\rangle$ [35]. We calculated the FCF based on the experimental potentials for this transition, which is 0.2515 ($|\langle v'|v\rangle|^2 = FCF$), and estimated the $\mu_e(R_c)$

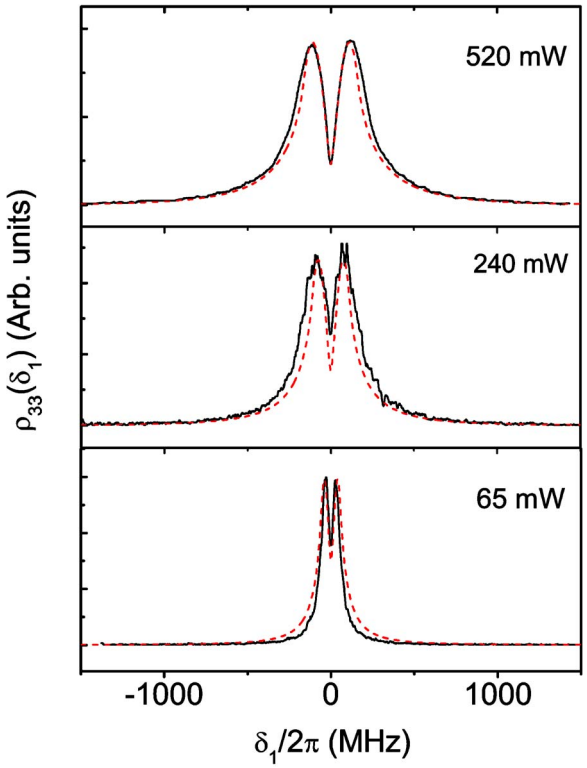

FIG. 5. (Color online) Measured fluorescence spectra of the upper level as a function of the probe laser detuning (δ_1) for different coupling laser power with the coupling laser frequency tuned at resonance ($\delta_2=0$). The fitting parameters are the same as in Fig. 4: $\langle v'|\mu_e|v\rangle=1.25(\pm0.2)$ a.u., $\gamma_{13}^c/2\pi=\gamma_{23}^c/2\pi=1$ MHz, $\gamma_{12}^c/2\pi=5$ MHz. (Solid lines: experimental, dashed lines: calculation.)

$\sim 2.5(\pm0.2)$ a.u. This value is slightly higher than our previous estimation (2.4 a.u.), but is still in a very good agreement with the *ab initio* calculations [23]. The main sources of uncertainty were the variation of the laser power and the uncertainty of the measurement of laser beam profiles. After completion of this step, we calculate the corresponding spectrum of ρ_{22}, which is again in good agreement with the experimental spectrum shown in Fig. 4(a) as a dashed line. However, the experimental dip is much narrower than the theoretical calculation. Both the theory and the experimental spectra clearly show that a strong coupling laser modified the transitions. The molecules stay in the ground state even though the laser ($L1$) was tuned to the resonance frequency of the first transition as long as the coupling laser ($L2$) couples the upper transition with adequate coupling strength (g_2). The optically opaque molecular gas now becomes transparent for laser $L1$ (EIT). Again, the dip is not due to the population transfer to the upper state $|3\rangle$ by the coupling laser $L2$, because the upper state has no population either. The fluorescence of both excited states becomes dark in the presence of the strong coupling laser. Keeping all parameters fixed and decreasing the strength of the coupling laser, we obtain the single peak OODR for ρ_{33} as shown by the dashed line in Fig. 3(b). The calculated ρ_{22} without the coupling laser is identical to the Doppler broadened profile as shown in Fig. 3(a).

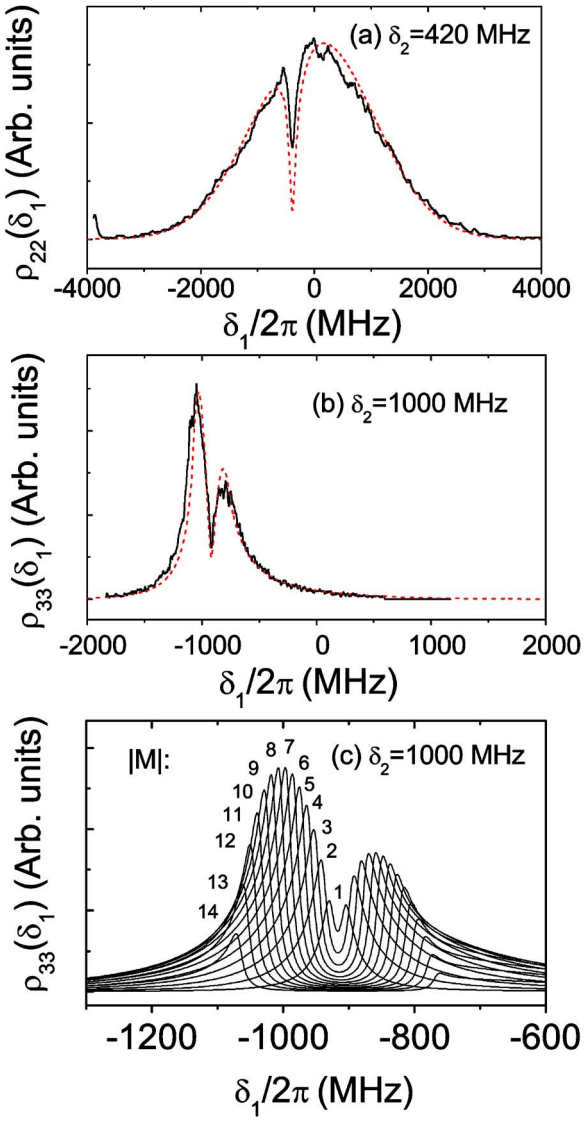

FIG. 6. (Color online) Fluorescence spectra for the coupling laser detuned from the resonance frequency: The coupling laser power is same as that in Fig. 4. (a) The coupling laser is detuned at $\delta_2/2\pi=420$ MHz above the resonance frequency. The EIT dip of level $|2\rangle$ shifted by 385 MHz below the resonance frequency. (b) The coupling laser is detuned 1.0 GHz above the resonance frequency. The splitting of the upper state $|3\rangle$ is still preserved, but shifted 917 MHz below the resonance frequency. (Solid lines: experiment, dashed lines: calculation) (c) Calculated 14 $|M|$ components of (b) before summation using Eq. (38).

As indicated in Eqs. (25) and (26) the Rabi frequency of the coupling field g_2 has a dominant influence on the depth and width of the dips of ρ_{33} once $g_2^2 \gg 4(\gamma_{21}+w)(\gamma_{31}+w)$. The decay rate of the upper level $|3\rangle$ and the branching ratios b_i, have a contribution to the depth of the dip of the spectra as well. The branching ratio b_i, the collision rate γ_{ij}^c and the transit rate w have a dominant contribution to the linewidth and the wings of the upper state spectra. This is understandable and expected compared to a closed system. A large γ_{ij}^c means that the coherence will be destroyed quickly, and a large transit rate w implies an effective shorter lifetime of the

excited levels, while small values of w and large branching ratios imply that the system is better described by a closed system. The dip of ρ_{22} is non zero since the P transition of the probe laser can populate the $M=0$ sublevel of $A\ ^1\Sigma_u^+$ state, while the coupling field transition is a Q transition, the $M=0$ level is decoupled from the coupling field transition [see Fig. 1(b)]. Also, Doppler broadening greatly reduces the width of the transparency window.

When the coupling laser is off resonance, the dips are still preserved as long as the coupling field is strong enough. Two experimental spectra with coupling laser detuned from the resonance by 420 MHz, and 1.0 GHz, respectively, while with the same laser intensity as in the Fig. 4 are shown in Figs. 6(a) and 6(b), which show that the coherence is robustly preserved. However, the position of the dips will change to the opposite direction of the detuning of the coupling field (δ_2). We can easily find, by checking the integral equation (34), that the position of the dip is at the modified two-photon transition $\delta_1=-|k_1/k_2|\delta_2$ due to the Doppler effect, and at $\delta_1=-\delta_2$ for Doppler free cases. This is a completely coherent process, since the detuning of $L2$ prevents the population buildup on level $|3\rangle$. The splitting of this component depends on the coupling field strength and the detuning of δ_2 as well as the linewidths of the two excited states. Furthermore, due to the magnetic sublevel degeneracy and the Doppler Effect, the resonance component of the upper level disappears and only the two-photon (two colors) component survives and splits as shown in Fig. 6(b). If we use the Eq. (1) in Ref. [22] to estimate the splitting of the upper state (ρ_{33}), the splitting should equal to 1096 MHz for the Rabi frequency of 450 MHz and the detuning of 1000 MHz for our experiment. However, our experiment result is about 244 MHz. This means that the simple model used in the above reference does not apply to our experiments. The theoretical calculations using our model concerning the 14 $|M|$ components clearly show the robustness of our theory and the calculations agree very well with the experimental spectra as shown in Fig. 6. We plot 14 $|M|$ sublevel components of Fig. 6(b) on an expanded scale to show the $|M|$-dependent splitting by using Eqs. (26) and (34) in Fig. 6(c). For a Q transition the splitting of each $|M|$ component is proportional to the value of $|M|$.

V. SUMMARY

In summary, we have observed the electromagnetically induced transparency (EIT) and dark fluorescence in an inhomogeneous broadened lithium molecular system. The power dependent upper state splitting spectrum provides a useful method to experimentally measure the transition dipole moment matrix element. The value of this parameter from fits of the experimental spectra agrees very well with the theoretical calculation. It could provide new insights into the electronic structures and dynamics of Rydberg states as discussed in Ref. [23]. The theoretical model in our work was developed for an open molecular system instead of using a closed system such as in Ref. [22]. In the process of fitting the experimental spectra we find that the branching ratio value can be varied over a large range but still give a reasonable fit. This implies that it is possible to observe EIT in a very open system, such as predissociated molecular states. Understanding predissociation of molecular states is very important for molecular dynamics studies and formation of molecules by inverse predissociation. We demonstrated that the coherence was remarkably preserved even when the coupling field was detuned far from the resonance. We have discussed a systematic approach to the treatment of the response of a three-level open molecular system to the presence of two laser fields. A simple closed three-level system model is not capable to explain the experimental results. Our theoretical model and the treatment of the degeneracy of the rotational levels, and inclusion of transient effects due to the finite size of laser beams agree very well with the experimental spectra.

ACKNOWLEDGMENTS

We thank Professors L. M. Narducci and F. C. Spano for valuable discussions, as well as A. Lazoudis, T. Kirova, and J. Magnes for their technical help in the lab. J. Qi is grateful for summer research support from Penn State University at Berks. We acknowledge support from NSF Grants Nos. PHY0245311 and PHY9983533 to Temple University.

[1] M. O. Scully and M. Fleishchhauer, Science **263**, 337 (1994).
[2] G. Vemuri, G. S. Agarwal, and B. D. Nageswara Rao, Phys. Rev. A **53**, 2842 (1996).
[3] R. Sussmann, R. Neuhauser, and H. J. Neusser, J. Chem. Phys. **103**, 3315 (1995); T. Halgmann and K. Bergmann, *ibid.* **104**, 7068 (1996).
[4] K. Ichimura, K. Yamamoto, and N. Gemma, Phys. Rev. A **58**, 4116 (1998).
[5] For a review of this subject, see E. Arimondo, in *Progress in Optics XXXV*, edited by E. Wolf (North-Holland, Amsterdam, 1996).
[6] H. Y. Ling, Y. Q. Li, and M. Xiao, Phys. Rev. A **53**, 1014 (1995).
[7] O. Schmidt, R. Wynands, Z. Hussein, and D. Meschede, Phys. Rev. A **53**, R27 (1996).
[8] S. E. Harris, Phys. Today **50**, 736 (1997).
[9] M. Fleischhauer and M. D. Lukin, Phys. Rev. Lett. **84**, 5094 (2000).
[10] S. A. Hopkins, E. Usadi, H. X. Chen, and A. V. Durrant, Opt. Commun. **138**, 185 (1997).
[11] N. E. Karapanagioti, O. Faucher, Y. L. Shao, D. Charalambidis, H. Bachau, and E. Cormier, Phys. Rev. Lett. **74**, 2431 (1995).
[12] L. V. Hau *et al.*, Nature (London) **397**, 594 (1999).
[13] M. M. Kash *et al.*, Phys. Rev. Lett. **82**, 5229 (1999); D. Budker, D. F. Kimball, S. M. Rochester, and V. V. Yashchuk, *ibid.*

83, 1767 (1999); M. D. Lukin, A. B. Matsko, M. Fleischhauer, and M. O. Scully, *ibid.* **82**, 1847 (1999).
[14] F. C. Spano, J. Chem. Phys. **114**, 276 (2001).
[15] F. Renzoni, A. Lindner, and E. Arimondo, Phys. Rev. A **60**, 450 (1999).
[16] J. Qi, G. Lazarov, X. Wang, L. Li, L. M. Narducci, A. M. Lyyra, and F. C. Spano, Phys. Rev. Lett. **83**, 288 (1999).
[17] R. Garcia-Fernandez, A. Ekers, J. Klavins, L. P. Yatsenko, N. B. Nikolai, B. W. Shore, and K. Bergmann, Phys. Rev. A **71**, 023401 (2005).
[18] F. Benabid, P. S. Light, F. Couny, and P. S. Russell, Opt. Express **13**, 5694 (2005).
[19] S. Ghosh, J. E. Sharping, D. G. Ouzounov, and A. L. Gaeta, Phys. Rev. Lett. **94**, 093902 (2005).
[20] F. Renzoni, W. Maichen, L. Windholz, and E. Arimondo, Phys. Rev. A **55**, 3710 (1997).
[21] A. Lazoudis, E. Ahmed, L. Li, T. Kirova, P. Qi, A. Hansson, J. Magnes, F. C. Spano, and A. M. Lyyra, quant-ph/0508110v1.
[22] M. A. Quesada, Albert M. F. Lau, David H. Parker, and David W. Chandler, Phys. Rev. A **36**, 4107 (1987).
[23] J. Qi, F. C. Spano, T. Kirova, A. Lazoudis, J. Magnes, L. Li, L. M. Narducci, R. W. Field, and A. M. Lyyra, Phys. Rev. Lett. **88**, 173003 (2002).
[24] F. S. Cataliotti, C. Fort, T. W. Hansch, M. Inguscio, and M. Prevedelli, Phys. Rev. A **56**, 2221 (1997).
[25] B. Laburthe Tolra, C. Drag, and P. Pillet, Phys. Rev. A **64**, 061401(R) (2001).
[26] U. Schloder, T. Deuschle, C. Silber, and C. Zimmermann, Phys. Rev. A **68**, 051403(R) (2003).
[27] S. Stenholm, *Foundations of Laser Spectroscopy* (Wiley Interscience, New York, 1984).
[28] W. Demtroder, *Laser Spectroscopy* (Spinger-Verlag, Berlin, 1982).
[29] Y. B. Band and P. S. Julienne, J. Chem. Phys. **94**, 5291 (1991).
[30] Y. B. Band and P. S. Julienne, J. Chem. Phys. **97**, 9107 (1992).
[31] S. Gerstenkorn *et al.*, *Atlas du Pectre d'absorption de la Molecule d'iode* (CNRS, Paris, 1978); S. Gerstenkorn *et al.*, Rev. Phys. Appl. **14**, 791 (1979).
[32] G. Baumgartner, H. Kornmeier, and W. Preuss, Chem. Phys. Lett. **107**, 13 (1984).
[33] A. Hansson (private communication).
[34] J. Sagle, R. K. Namioka, and J. Huennekens, J. Phys. B **29**, 2629 (1996).
[35] J. Brooke Koffend, R. Bacis, and Robert W. Field, J. Chem. Phys. **70**, 2366 (1979).